Analysis of neutrinos emitted by radioactive ${}^{40}_{19}K$ in the earth's core

A thesis submitted in partial fulfillment of the requirements for the degree of Bachelor of Science in Physics from the College of William and Mary in Virginia.

By M. Audrey Lukito

Williamsburg, VA

November 11, 2004

This thesis is dedicated to my beloved parents, Budi and Angela Loekito, for their loving support at all times

and

to my advisor Dr. Sher, without whose help and guidance the completion of this work would be impossible

Abstract

This thesis analyzes neutrinos emitted by radioactive particles, mainly ${}^{40}_{19}K$, in the earth's core. For the detector, we use data from the Borexino detector (which is currently being built), a detector for low-energy neutrinos. We calculated the number of neutrinos that could be detected (after taking into account the various possible concentrations of potassium in the core) and compared that number to the detector's background impurities. Then we analyzed the case of neutrino flavor oscillations and calculated their transition probabilities. Finally, we discussed how the detection of these neutrinos could offer us more insight into the currently very limited knowledge of the earth's core.

Table of Contents

1) Introduction

The discovery of the neutrino dates back to 1930, when physicists discovered a problem in nuclear beta decay (*i.e.* the process where a radioactive nucleus is transformed into a slightly lighter nucleus with the emission of an electron, or "beta ray"). Since this is a two-body process, by the law of the conservation of energy, the outgoing energies (that of the lighter nucleus and the electron) should be fixed; but experiments proved that the emitted electrons possessed a continuous spectrum of energies. Wolfgang Pauli proposed in 1931 that a neutral particle was emitted along with the electron, and this particle is what carries the "missing energy". A few years later Fermi presented a theory of beta decay which incorporates Pauli's particle, which he called the neutrino [1].

Neutrinos are electrically neutral, spin ½ particles which interact very weakly with matter through the weak nuclear and gravitational forces. There are three flavors of neutrino corresponding to three massive leptons, *i.e.* the electron neutrino, the tau neutrino and the muon neutrino.

It was previously thought that neutrinos are massless, but the Solar Neutrino problem (SNP) indicated that this assumption is false. The problem was first identified in 1968 when Davis, Harmer and Hoffman published results of their first solar neutrino detection experiment [2]. The detector was a 100,000 gallon tank of detergent buried a mile deep in South Dakota. Electron neutrinos from the sun interact with Chlorine atoms in the tank, producing radioactive argon and electrons. When they counted the electrons, they calculated the solar neutrino flux to be 1/3 of what theorists predicted it should be. Subsequent experiments also produce results showing that the flux is much less than theoretical predictions.

This problem finally revealed the fact that the neutrino mass eigenstates are not identical to the flavor states, and that they are not all degenerate (*i.e.* neutrinos are not massless), thus allowing for flavor oscillations. In the case of SNP, some of the electron neutrinos coming from the sun become muon neutrinos; and since they were undetectable in the above-mentioned experiments, the observable signal decreased. Current detectors are far more advanced and many can detect different flavors of neutrinos. In this project we are using data from the Borexino detector[1], a real-time detector that can detect low-energy electron neutrinos. It is currently under construction and is built primarily to (but its function is not limited to) detect solar neutrinos from the ^{7}Be reaction chain. In this research we will use it to detect neutrinos produced by $^{40}_{19}K$, the primary radioactive material in the earth's core.

In the course of this paper, we will first look at the concept of neutrino flavor oscillations, both in vacuum and in matter of constant and variable densities. Then we shall get into the actual research: first, c the existence and abundance of $^{40}_{19}K$ in the core producing the electron neutrinos, the rate and energies of the reactions, and the probability of their detection by Borexino (whose properties, *e.g.* radiopurity, sensitivity, *etc.* shall also be discussed). We shall first consider the case where there is no oscillation and analyze possible background problems, and then go on to the case of neutrino oscillations and calculate the number of muon neutrinos we can expect to be detected, then discuss the results.

[1] Data for the properties of Borexino (currently being built) in this paper are mainly found from the web sites of various research projects who are doing experiments with the detector.

2) Theory of neutrino oscillations

2.1) Vacuum oscillations

Here we shall discuss how neutrinos oscillate in vacuum; a somewhat similar discussion can also be found in Bernstein and Parke [3].

Consider a two-neutrino system. A neutrino wavefunction $\vec{\nu}$ in the mass basis can be written as:

$$\vec{\nu}(t) = \nu_1(t)\,|\nu_1> + \nu_2(t)\,|\nu_2> \qquad \{1\}$$

where 1 and 2 are the mass eigenstates labels, with 1 signifying the state which is mostly electron, and 2 for the state which is mostly muon. Since neutrinos move at a speed close to c, we can use the Dirac equation (the relativistic form of the Schrodinger equation); in the mass basis, with $c=\hbar=1$, this reduces to:

$$i\frac{\partial}{\partial t}\begin{pmatrix}\nu_1\\ \nu_2\end{pmatrix} = \begin{pmatrix}\sqrt{K^2+m_1^2} & 0\\ 0 & \sqrt{K^2+m_2^2}\end{pmatrix}\begin{pmatrix}\nu_1(0)\\ \nu_2(0)\end{pmatrix} \qquad \{2\}$$

where K is the momentum of the neutrino state.

To simplify our calculation, we can expand the diagonal elements in {2} in Taylor series:

$$\sqrt{K^2+m_i^2} = K + \frac{m_i^2}{2K} + \dots \qquad \{3\}$$

plus higher order terms, which may be discarded in our ultrarelativistic case. If we define an (intrinsically positive) quantity $\Delta m_0^2 = m_2^2 - m_1^2$, we can re-express {3} as:

$$\sqrt{K^2+m_i^2} = \left(K + \frac{m_1^2+m_2^2}{4K}\right) \pm \frac{\Delta m_0^2}{4K} \qquad \{4\}$$

taking the plus sign for the 1 state and the minus sign for the 2 state. Since the bracketed term in {4} appears in both terms in the Hamiltonian, we can discard it, since the overall phase of a wavefunction doesn't matter. Then we get:

$$i\frac{\partial}{\partial t}\begin{pmatrix}\nu_1\\ \nu_2\end{pmatrix}=\frac{\Delta m_0^2}{4K}\begin{pmatrix}-1 & 0\\ 0 & 1\end{pmatrix}\begin{pmatrix}\nu_1(0)\\ \nu_2(0)\end{pmatrix} \qquad \{5\}$$

which can easily be solved for the neutrino wavefunction, *i.e.*

$$\vec{\nu}\,(\mathrm{t})=\begin{pmatrix}Exp\left(i\frac{\Delta m_0^2}{4K}t\right) & 0\\ 0 & Exp\left(-i\frac{\Delta m_0^2}{4K}t\right)\end{pmatrix}\begin{pmatrix}\nu_1(0)\\ \nu_2(0)\end{pmatrix} \qquad \{6\}$$

Flavor oscillations are caused by the differences between the flavor and mass bases, which are related by a rotation matrix:

$$\begin{pmatrix}\nu_e(\tau)\\ \nu_\mu(\tau)\end{pmatrix}=\begin{pmatrix}\cos(\theta_0) & -\sin(\theta_0)\\ \sin(\theta_0) & \cos(\theta_0)\end{pmatrix}\begin{pmatrix}\nu_1(\tau)\\ \nu_2(\tau)\end{pmatrix} \qquad \{7\}$$

where θ_0 is the vacuum mixing angle, which is taken to be less than $\frac{\pi}{2}$. Note that the mixing angle θ obtained when a rotation matrix like {7} acts on a matrix of the form $\begin{pmatrix}A & C\\ C & B\end{pmatrix}$ is given by the relation $C=\frac{A-B}{2}Tan(2\theta)$.

When we apply the rotation {7} to {6}, we get an expression for the neutrino in the flavor basis, *i.e.*

$$\vec{\nu}(t)=\begin{pmatrix}\nu_e(t)\\ \nu_\mu(t)\end{pmatrix}=\begin{pmatrix}\sqrt{1-\sin^2(2\theta_0)\sin^2(1.27\frac{\Delta m_0^2}{K}L)} & \sin(2\theta_0)\sin(1.27\frac{\Delta m_0^2}{K}L)\\ \sin(2\theta_0)\sin(1.27\frac{\Delta m_0^2}{K}L) & \sqrt{1-\sin^2(2\theta_0)\sin^2(1.27\frac{\Delta m_0^2}{K}L)}\end{pmatrix}\begin{pmatrix}\nu_e(0)\\ \nu_\mu(0)\end{pmatrix} \{8\}$$

where L (the distance traveled by the neutrino) is defined as $L=ct$. Here $\Delta m_0^{\ 2}$ is expressed in units of eV^2, L in kilometers, and energy in MeV. Thus here we can know the probability of neutrino oscillation between flavors: For example, the probability that an electron neutrino will oscillate into a muon neutrino at a later time t is $P_{e\to\mu} = \left\langle \nu_\mu(t) \middle| \nu_e(0) \right\rangle^2$, and similarly, the probability of a muon turning into an electron neutrino is $P_{\mu\to e} = \left\langle \nu_e(t) \middle| \nu_\mu(0) \right\rangle^2$. Both of these probabilities can be easily obtained from {8}; *i.e.* they refer to the square of the off-diagonal elements of the Hamiltonian. Hence the probability of transition between flavors for neutrinos oscillating in vacuum is:

$$P_{trans} = \sin^2(2\theta_0)\sin^2(1.27\frac{\Delta m_0^2}{K}L) \qquad \{9\}$$

Note that the second $\sin^2$ term in {9} is a function of the distance traveled by the neutrino; the resonance length L_{res} is the distance that maximizes this term, and hence P_{trans}:

$$L_{res} = 1.24\left(\frac{\Delta m_0^2}{K}\right)^{-1} \qquad \{10\}$$

In the case where many neutrinos are generated at different places spanning a distance much longer than L_{res}, however, this term averages to ½.

2.2) Matter oscillations

Neutrinos oscillate somewhat differently in matter. Flavor oscillations are somewhat enhanced—an effect called the MSW (Mikheyev, Smirnov, Wolfenstein) effect. To analyze this, let us first obtain the Dirac equation for the flavor basis by applying the rotation {7} to {6}:

$$i\frac{\partial}{\partial t}\begin{pmatrix}\nu_e\\ \nu_\mu\end{pmatrix}=\frac{\Delta m_0^2}{2K}\begin{pmatrix}-\cos(2\theta_0) & \sin(2\theta_0)\\ \sin(2\theta_0) & \cos(2\theta_0)\end{pmatrix}\begin{pmatrix}\nu_e(0)\\ \nu_\mu(0)\end{pmatrix} \qquad \{11\}$$

In matter, it is necessary to add a term proportional to the electron density of the medium to the top diagonal element of the Hamiltonian in {8} (*i.e.* the flavor basis):

$$+\sqrt{2}G_F N_e \qquad \{12\}$$

where G_F is the Fermi coupling constant, and N_e is the number density of electrons in the medium. In the case of a medium of constant density, N_e is constant. Then equation {8} becomes:

$$i\frac{\partial\nu}{\partial t}=\frac{1}{2}\begin{pmatrix}-\frac{\Delta m_0^2}{K}\cos(2\theta_0)+2\sqrt{2}G_F N_e & \frac{\Delta m_0^2}{K}\sin(2\theta_0)\\ \frac{\Delta m_0^2}{K}\sin(2\theta_0) & \frac{\Delta m_0^2}{K}\cos(2\theta_0)\end{pmatrix}\begin{pmatrix}\nu_e(0)\\ \nu_\mu(0)\end{pmatrix} \qquad \{13\}$$

This equation can be simplified if we change the overall phase of the wavefunction by subtracting one half of the added term from the diagonals, yielding:

$$i\frac{\partial\nu}{\partial t}=\frac{1}{2}\begin{pmatrix}-\frac{\Delta m_0^2}{K}\cos(2\theta_0)+\sqrt{2}G_F N_e & \frac{\Delta m_0^2}{K}\sin(2\theta_0)\\ \frac{\Delta m_0^2}{K}\sin(2\theta_0) & \frac{\Delta m_0^2}{K}\cos(2\theta_0)-\sqrt{2}G_F N_e\end{pmatrix}\begin{pmatrix}\nu_e(0)\\ \nu_\mu(0)\end{pmatrix} \qquad \{14\}$$

So we see that here we get an equation very similar to {11}, namely with diagonal terms which are equal in magnitude but opposite in sign, and with identical off-diagonal terms. Hence we know that this matrix is also diagonalizable; specifically, we can define a matter mixing angle θ_N and a matter squared-mass difference Δm_N^2 by

$$\begin{aligned}\frac{\Lambda m_N^2}{K}\cos(2\theta_N)&=\frac{\Delta m_0^2}{K}\cos(2\theta_0)-\sqrt{2}G_F N_e\\ \frac{\Lambda m_N^2}{K}\sin(2\theta_N)&=\frac{\Delta m_0^2}{K}\sin(2\theta_0)\end{aligned} \qquad \{15\}$$

Solving for θ_N and Δm_N^2, we get:

$$\theta_N = \frac{1}{2}\arctan\left(\frac{1}{\cot\left(2\theta_0\right) - \frac{\sqrt{2}KG_F N_e}{\Delta m_0^2 \sin\left(2\theta_0\right)}}\right)$$

$$\Delta m_N^2 = \Delta m_0^2 \frac{\sin(2\theta_0)}{\sin(2\theta_N)} \qquad \{16\}$$

Maximal mixing, or resonance, happens when the off-diagonal terms in {14} is minimum, *i.e.* when $\theta_N = \frac{\pi}{4}$; or, plugging this value for θ_N in {16}:

$$N_{e\_resonance} = \frac{\Delta m_0^2 \cos\left(2\theta_0\right)}{\sqrt{2}KG_F} \qquad \{17\}$$

The solution for the Dirac equation {14} is given by {8}, and the transition probability is also identical to {9}, except that $\Delta m_0^2, \theta_0$ is replaced by their matter analogs $\Delta m_N^2, \theta_N$.

In a medium of non-constant density, the electron density will be some function of time, *i.e.* $N_e(t)$. Hence now the mixing angle and squared-mass difference will also depend on time; so we have to obtain the time-dependent wavefunction $\vec{v}$ solely in the flavor basis, since the rotation matrix relating the flavor and mass bases is now some unknown function of time. The Dirac equation {14} thus becomes:

$$i\frac{\partial \nu}{\partial t} = \frac{1}{2}\begin{pmatrix} -\frac{\Delta m_0^2}{K}\cos(2\theta_0) + \sqrt{2}G_F N_e(t) & \frac{\Delta m_0^2}{K}\sin(2\theta_0) \\ \frac{\Delta m_0^2}{K}\sin(2\theta_0) & \frac{\Delta m_0^2}{K}\cos(2\theta_0) - \sqrt{2}G_F N_e(t) \end{pmatrix}\begin{pmatrix} \nu_e(0) \\ \nu_\mu(0) \end{pmatrix} \qquad \{18\}$$

Assuming that the mixing angle changes adiabatically, we get

$$\nu(t) = Exp\left(-i\int H(t)dt\right)\nu(0) \qquad \{19\}$$

where *H(t)* is the Hamiltonian in {18}. If the electron density can be expressed as an analytic function of time, *H(t)* can be integrated term by term:

$$J(t)=\int H(t)dt=\frac{t}{2}\begin{pmatrix} -\frac{\Delta m_0^2}{K}\cos(2\theta_0)+\sqrt{2}G_F\frac{\int N_e(t)dt}{t} & \frac{\Delta m_0^2}{K}\sin(2\theta_0) \\ \frac{\Delta m_0^2}{K}\sin(2\theta_0) & \frac{\Delta m_0^2}{K}\cos(2\theta_0)-\sqrt{2}G_F\frac{\int N_e(t)dt}{t} \end{pmatrix} \quad \{20\}$$

This matrix is diagonalizable; in fact, we can define $\Delta m_N^2(t), \theta_N(t)$ very similar to {16}:

$$\theta_N\,(\mathrm{t}) = \frac{1}{2}\arctan\left(\frac{1}{\cot\left(2\theta_0\right)-\frac{\sqrt{2}KG_F\int N_e(t)dt}{\Delta m_0^2 t\sin\left(2\theta_0\right)}}\right)$$

$$\Delta m_N^2\,(\mathrm{t}) = \Delta m_0^2\frac{\sin(2\theta_0)}{\sin(2\theta_N(t))} \quad \{21\}$$

A problem arises when we try to solve for $\vec{\nu}$ (t), since the term in the exponential in {19} contains off-diagonal elements. We can solve this problem by knowing that for a matrix *A* similar to a diagonal matrix *D*, *A*=*SD* S^{-1}, where *S* is the rotation matrix. By approximating functions of matrices by their Taylor expansions, we get:

$$e^A = Se^D S^{-1} \quad \{22\}$$

Applying {22} to {19} gives us the solution:

$$\vec{\nu}\,(\mathrm{t}) = \begin{pmatrix} \cos\left(\theta_N(t)\right) & -\sin\left(\theta_N(t)\right) \\ \sin\left(\theta_N(t)\right) & \cos\left(\theta_N(t)\right) \end{pmatrix} \begin{pmatrix} Exp\left(i\frac{\Delta m_N^2(t)}{4K}t\right) & 0 \\ 0 & Exp\left(-i\frac{\Delta m_N^2(t)}{4K}t\right) \end{pmatrix} \begin{pmatrix} C & S \\ -S & C \end{pmatrix} \vec{\nu}(0)$$

$$= \begin{pmatrix} \sqrt{1-\sin^2\left(2\theta_N(t)\right)\sin^2(1.27\frac{\Delta m_N^2(t)}{K}L)} & \sin(2\theta_N(t))\sin(1.27\frac{\Delta m_N^2(t)}{K}L) \\ \sin(2\theta_N(t))\sin(1.27\frac{\Delta m_N^2(t)}{K}L) & \sqrt{1-\sin^2\left(2\theta_N(t)\right)\sin^2(1.27\frac{\Delta m_N^2(t)}{K}L)} \end{pmatrix} \vec{v}(0) \quad \{23\}$$

which is very similar to {8}; in fact, there are two ways to obtain $\vec{v}$(t): By solving in the mass basis first, as Bernstein and Parke did in {8}, or by the method just discussed. Generally we can always solve for $\vec{v}$(t), except in resonance cases, where adiabaticity fails.

3) Analysis of neutrinos

3.1) The core and its radioactive elements

We are now ready to analyze the behavior and detection of neutrinos generated in the earth's core. The earth's mass is 5.97 x10^{24} kg, with the core consisting primarily of iron and some nickel [4] and having a mass 32% of the earth's [5], *i.e.* about 1.91x10^{24} kg.

It was traditionally thought that the core is composed primarily of iron with small amounts of nickel and other elements [5, 6]. Over 30 years ago it was theoretically suggested that a significant amount of radioactive potassium is also present, acting as a substantial heat source. Very recently this idea has resurfaced as various experimental evidence backs up the theoretical possibility [7, 8, 9, 10]. Lee and Jeanloz, for example, proves by high-resolution x-ray diffraction that potassium (K) alloys with iron (Fe) when they're heated together at high pressure[9]. The estimated abundance of K in the core widely varies, from 60-330 ppm [10], 240 ppm [11], 1200 ppm [8], to 7000 ppm [9], which all sources generally agree to be the maximum possible amount. In this project we shall first assume the maximum limit of 7000 ppm, and see whether the neutrinos generated will be significant enough for detection and data analysis. We shall also assume that K is the sole radioactive element in the core, since that seems to be the only possible case right now, although some do not close the possibility of future evidence suggesting that radioactive U and Th are also present in the core [9].

3.2) The detector and its properties

The Borexino detector is an unsegmented liquid detector for low energy (below 1 MeV) neutrinos, featuring 300 tonnes of well-shielded ultrapure scintillator and 2200 photomultipliers [12], see Fig. 1. The inner scintillator, where the neutrinos interact (*i.e.* scatter from electrons) and are detected, has a radius of about 1.7 m, or a volume of 20.58 m^3. The scintillator mixture is made of pseudocum (PC) and 1.5 g/l of PPO, whose average density is roughly equal to water (n= 3x 10^{30} electrons/m^3), which is what we'll use in this project.

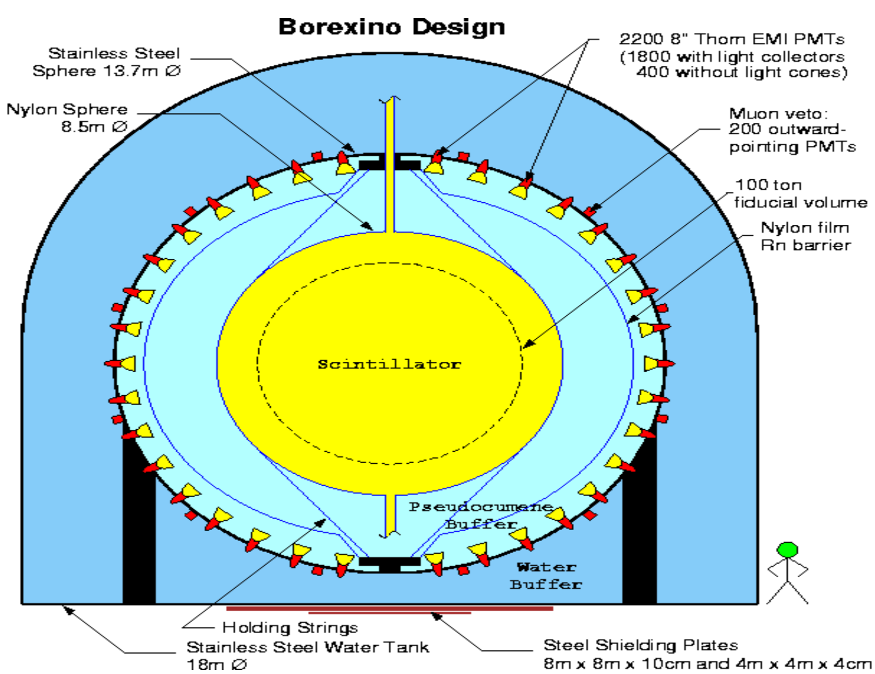

Figure 1. The Borexino detector. Specifically designed for low energy neutrinos, it features 300 tonnes of ultrapure scintillator made of pseudocum and PPO, where the neutrinos interact.

To calculate the detector's efficiency, we compare the number of solar neutrinos (coming from the monoenergetic 0.86 MeV ^{7}Be chain) that *should* be detected by Borexino (considering its size, density, electron's cross section, *etc.*) if its efficiency were 100% to the number that it expects to detect, which is 43.3/day using the Standard Solar Model [13]. From the solar neutrino spectrum (see Fig. 2), the flux for these neutrinos is N=5x10^{13}/m^2/s. The neutrino cross section for the scattering $\nu_e + e^- -> \nu_e + e^-$ is $\sigma_\nu = 9.5x10^{-49} E_\nu \left(\frac{m^2}{MeV}\right)$ [3], where E_ν is the neutrino's energy (0.86 MeV in this case).

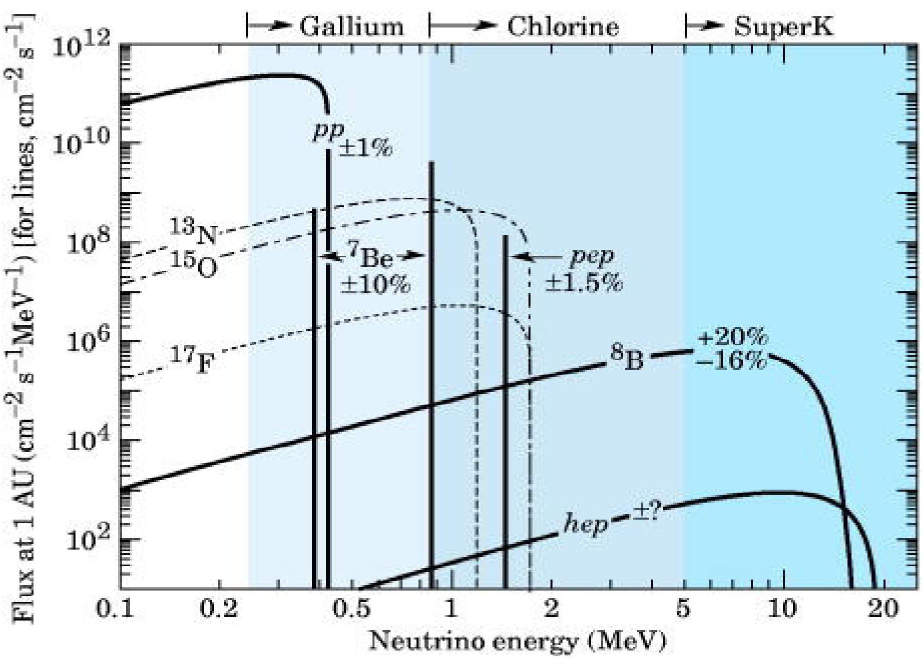

Figure 2. The solar neutrino spectrum. Although Borexino is a multipurpose low-energy neutrino detector, it is originally designed to detect neutrinos coming from the monoenergetic 0.86 MeV ^{7}Be chain coming from the sun. We use the available data for neutrino detection from this chain to calculate the detector's efficiency.

So the average distance traveled by the neutrino is given by

$$\lambda = \frac{1}{(n)(\sigma_\nu)} \qquad \{24\}$$

which, in this case, is λ=4x10^{17} m. If the detector has 100% efficiency, then the number of neutrinos detected per second would be related by:

$$\Sigma = \frac{(N)(Vol)}{\lambda} \qquad \{25\}$$

where *Vol* is the scintillator's volume in m^3. In our case, that means that we would get 0.00257 neutrinos/s, or 222 neutrinos/ day. Using the standard solar model (SSM), however, Borexino is expected to detect 43.31 events/day [15]; so roughly, the detector's efficiency is around 19%.

We must also remember that besides detecting neutrinos coming from the core, Borexino will also detect neutrinos generated in its own scintillator by radioactive elements (this is background). Scientists at Gran Sasso Laboratory establish that this radioactive impurity is at most 10^{-9} Bq/kg scintillator due to the decay products of U and Th. The 300-tonne scintillator will thus have a 0.0003 Bq impurity; *i.e.* the background will produce around 26 electrons/ day. Borexino's main laboratory at Gran Sasso estimated the energy of the background particles to be between 0.25-0.8 MeV, which is similar to the range of the energy of the neutrinos from the core (see discussion below). We shall see whether the background is too high by comparing it with the number of neutrinos generated in the core detected by Borexino.

3.3) Neutrino detection, assuming zero oscillation

For this first case we shall disregard any possible flavor oscillations. A concentration of 7000 ppm means that there's about 13.4x10^{24} g of K, or about 2x10^{47} K atoms in the core. With a half life of 1.25 billion years, that would give us 2.54x10^{30} decays/s. There are two modes of decay for potassium [4], the first one being $^{40}_{19}K$ **->**

${}^{40}_{20}Ca + e^- + \overline{\nu}_e$ (89.28% occurrence likelihood and reaction energy of 1.311 MeV) and the second one being ${}^{40}_{19}K + e^- -> {}^{40}_{18}Ar + \nu_e$ (10.72% likelihood, reaction energy of 2.01 MeV). The latter case would be interesting, since the neutrino is monoenergetic, but unfortunately the energy is too high for Borexino to detect. So we will analyze the first case, which is a Beta decay, where the (anti)neutrino has a maximum energy of 0.8 MeV. This means that there will be 2.27x10^{30} detectable decays/s. With the earth's mean radius being 6.37x10^{6} m, we shall get about 4.45x10^{15} decays/s/m^{2}. The cross section for the antineutrinos generated in this decay (which are detected through electron scattering) is $\sigma_{\overline{\nu}} = 4x10^{-49} E_\nu \left(\frac{m^2}{MeV} \right)$ [3], so by {24} we shall get $\lambda(E_\nu) = \frac{8.3x10^{17}}{E_\nu} \left(\frac{m}{MeV} \right)$, where E_ν is the energy of the antineutrino, ranging from 0 to 0.8 MeV. DeBenedetti [16] gives us the relation for the momentum distribution of the electron in beta decay:

$$N_e dp_e = \left(\frac{16\pi^2}{h^6 c^3} \right) p_e^2 (E_0 - E_e)^2 dp_e \qquad \{26\}$$

where N_e is the number of electrons with momentum p_e and energy E_e, and E_0 is the total energy (electron plus antineutrino). The bracketed term in {26} is a constant, it can be easily scaled to unity. With the knowledge that $E_0 = E_e + E_\nu$=1.311 MeV, with $E_e = \sqrt{p_e^2 + m_e^2}$ (where m_e=0.511 MeV/c) and that $E_\nu \approx p_\nu$ (due to the slight mass of neutrinos), we can easily obtain the energy distribution for the antineutrinos, *i.e.*

$$N_\nu(E_\nu) = E_\nu^2 \left((1.311 - E_\nu)^2 - 0.511^2 \right) dE_\nu \qquad \{27\}$$

The probability that an antineutrino will be detected by Borexino every second, taking all these things into account, would then be:

$$P = (Vol)(Dec)(Eff)\int_{0.0}^{0.8MeV} \frac{N_\nu}{\lambda(E_\nu)} dE_\nu \qquad \{28\}$$

Where *Vol*= volume of detector's scintillator=20.58 m^3, *Dec*=number of decays/s/m^2 = $4.45\text{x}10^{15}$, and *Eff*=efficiency of detector=19%. The integral is very simple to calculate, since $1/\lambda(E_\nu)$ is just a linear function of the energy. Calculating {28} gives us *P*=$4.42\text{x}10^{-4}$ antineutrinos/s; *i.e.* we should be able to detect about 38.2 antineutrinos/day.

These neutrinos, however, will all come at different angles, and we wish to make the plot of the number of neutrinos versus the cosine of the angle α they come at (see Fig. 3 below).

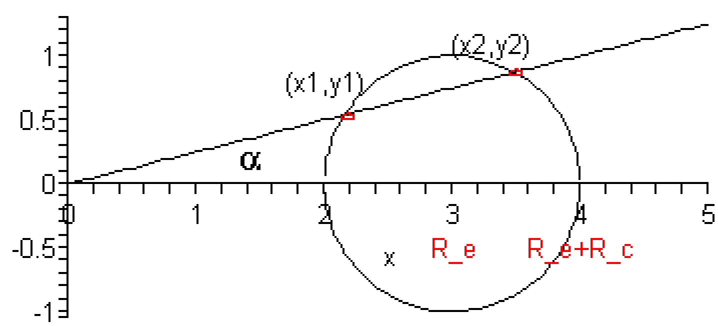

R_e=radius of the earth
R_c=radius of the core

Figure 3. Schematic diagram of the earth's core and angle of incident neutrinos

The volume of the shell between α and α+dα can be calculated using the relationships:

$$\begin{aligned} (x_1 - R_E)^2 + y_1^2 &= R_c^2 \\ (x_2 - R_E)^2 + y_2^2 &= R_c^2 \\ \frac{y_1}{x_1} = \frac{y_2}{x_2} &= \tan\alpha \end{aligned} \qquad \{29\}$$

where R_E is the earth's radius, and R_C is the core's radius.

The number of neutrinos detected at angle α is proportional to this volume:

$$V(\alpha) = \pi(y_2^2 - y_1^2)\csc\alpha = \pi\left\{R_E^2 \sin^2(2\alpha) + 2R_E(\cos(2\alpha) - 1)x_1\right\}\csc\alpha, \qquad \{30\}$$

where

$$x_1 = \frac{R_E - \sqrt{R_C^2 \sec^2\alpha - R_E^2 \tan^2\alpha}}{\sec^2\alpha} \qquad \{31\}$$

with the constraint that $\alpha < \arcsin(\frac{R_C}{R_E}) \approx 0.5762$ radians.

Or, in terms of cos α:

$$V(\cos\alpha) = 4R_E\pi\cos\alpha\sqrt{(1-\cos^2\alpha)\left\{R_C^2 - R_E^2(1-\cos^2\alpha)\right\}} \qquad \{32\}$$

This equation is plotted in Fig. 4. The use of Simpson's rule in calculating the integral of *V(cos* α *)* gives us 9.8 $\times 10^{13}$. Since there are 13,943 neutrinos detected/year, multiplying {32} by $\frac{13943}{9.8x10^{13}}$ gives us the normalized graph, *i.e.* the plot of the number of neutrinos detected/year as a function of $\cos\alpha$ (see Fig. 5).

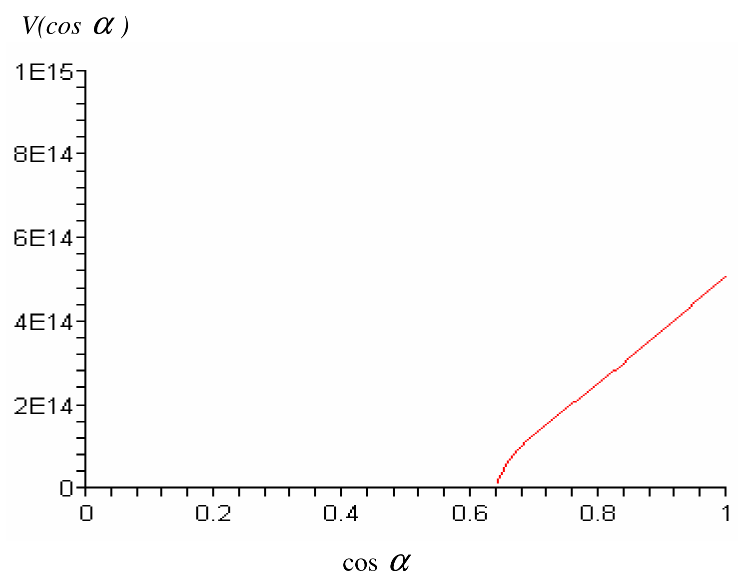

Figure 4. Plot of *V(cos* α *)*, which is proportional to the numbers of neutrino detected by Borexino.

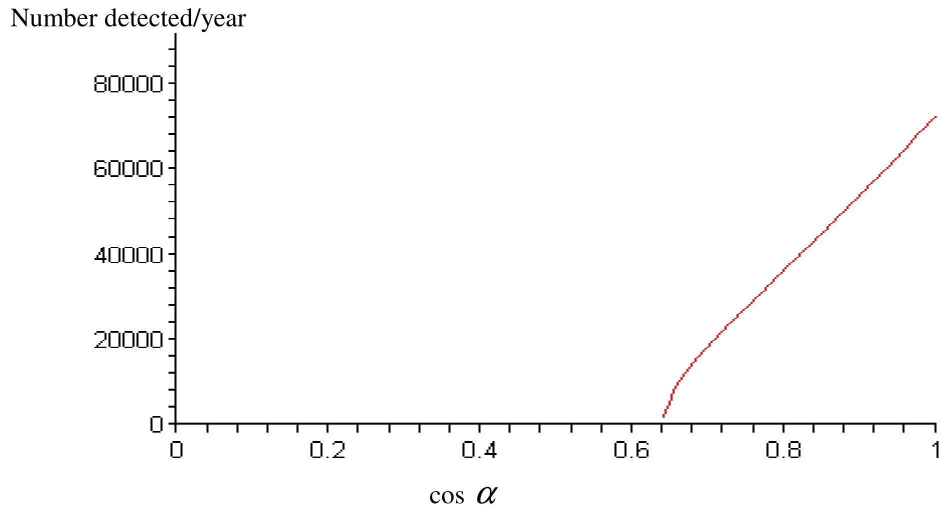

Figure 5. Number of neutrinos detected/year (from the core) as a function of cos α

This plot is based, of course, on the assumption that the concentration of K in the core is 7000 ppm (the maximum postulated amount). We wish to see how $N(\cos\alpha)$ varies at concentrations of 7000, 4000, 2000, 1000, 500 and 100 ppm and see at which point the neutrinos coming from the core becomes indistinguishable from the background, see Fig. 6. In this figure we can see that the difference between background and core-produced neutrinos begin to blur at around 500 ppm. This means that speculated potassium concentrations of 60-330 ppm [10] or 240 ppm [11] will not be significant enough to produce well-detected neutrinos using Borexino.

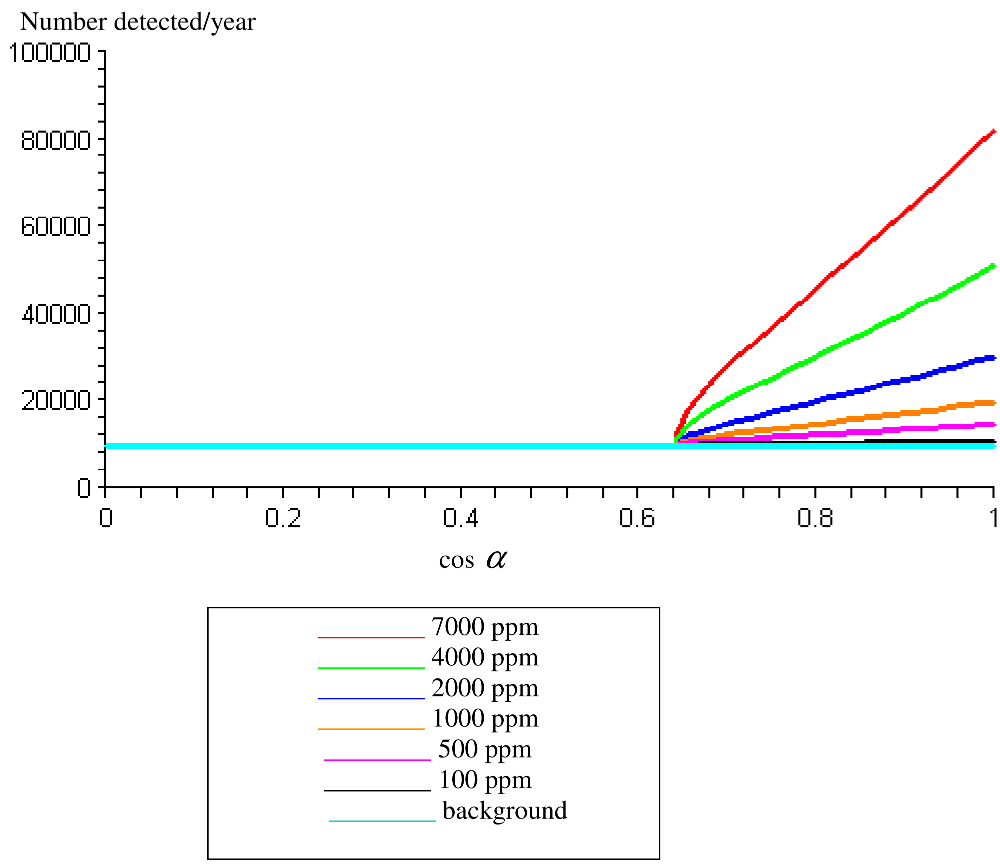

Figure 6. Number of neutrinos detected/year as a function of cos α at various concentrations of radioactive K in the core.

3.4) Neutrino detection with flavor oscillations

When we take flavor oscillations into account, we need to know the density of the earth through which the neutrino travels; since the probability of flavor transitions depend on this. According to Bullen [17], there are various models of the earth's density: For our work, we are going to use his B_2 model (see Table 1 for the table and Fig. 7 the graph). The earth's core, as mentioned before, is composed primarily of iron (Fe; 56 g/mol, 26 electrons/atom); while the mantle, according to Palme and O'Neill [18], is composed primarily of MgO (36%; 40g/mol, 20 electrons/atom) and SiO_2 (51%; 60g/mol, 30 electrons/atom). So the mantle (depth up to 2900 km) has an electron concentration of about 3×10^{23} electrons/g while the core has a concentration of 2.8×10^{23} electrons/g.

Table 1. The earth density as a function of depth from the surface (data is from Bullen's B2 model)

Earth density (g/cm^3)	Depth from the surface (km)
3.32	33
3.51	245
4.49	984
5.06	2000
5.4	2700
5.69	2886
11.39	4000
11.87	4560
12.3	4710
12.74	5160
13.03	6371

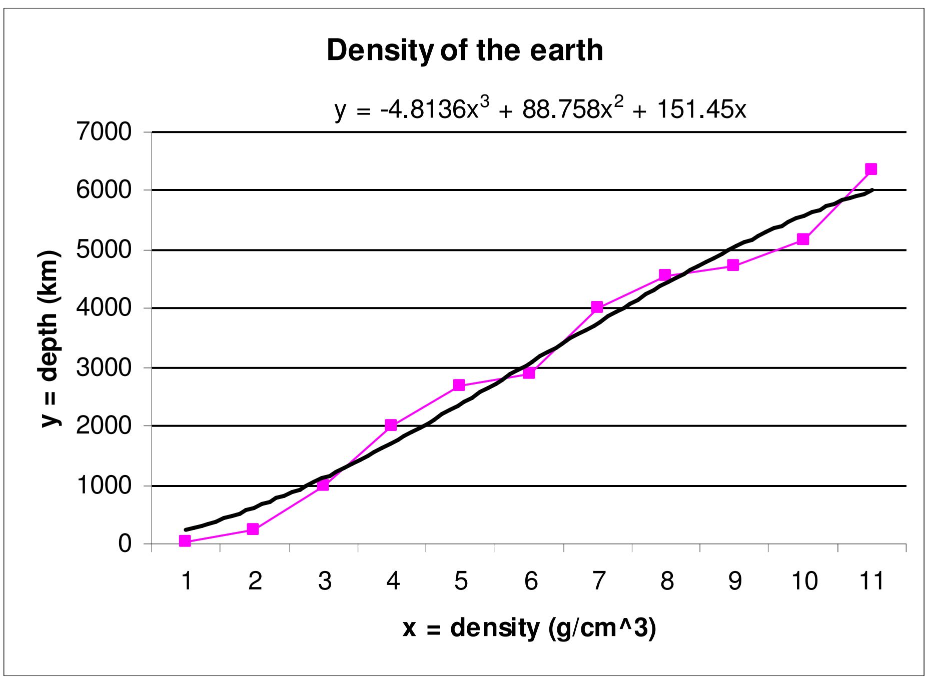

Figure 7. Plot of Bullen's B2 model of the earth's density

Using the relation that time (in s) is $t = \frac{L}{c} = \frac{(6371km - depth)x10^3}{3x10^8 m/s}$ (the *depth* is in km) and the data in table 1, we get a table of electron density values vs. time and its graph (see Table 2 and Fig. 8).

Table 2. Electron density as a function of time elapsed since neutrinos leave the earth's core.

Time (s)	Electron density (m^{-3})
0.00E+00	3.91E+30
4.04E-03	3.82E+30
5.37E-03	3.69E+30
6.04E-03	3.56E+30
7.90E-03	3.42E+30
1.16E-02	1.59E+30
1.22E-02	1.51E+30
1.46E-02	1.42E+30
1.80E-02	1.26E+30
2.04E-02	9.83E+29
2.11E-02	9.30E+29

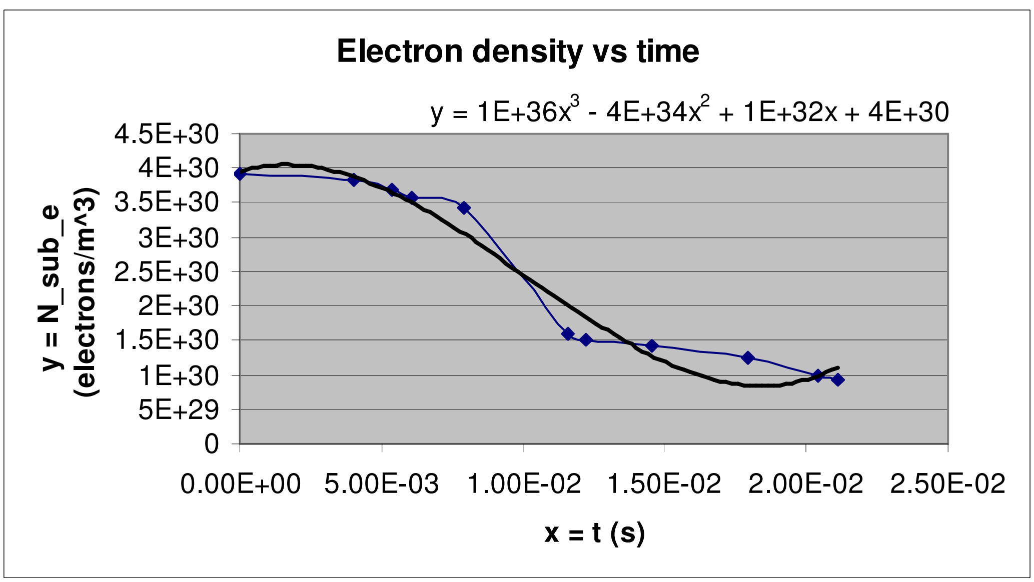

Figure 8. Plot of electron density as a function of time (*i.e.* the time that has elapsed since the neutrinos start out from the core of the earth).

Now we are ready to calculate the transition probability, using {21} and {23}. These equations, however, are not in their proper units, so we need to multiply them by a conversion factor. In {21}, for instance, the expression $\frac{\sqrt{2}KG_F \int N_e(t)dt}{\Delta m_0^2 t}$ needs to be dimensionless. In our data (since we assumed that c is unity throughout our equations) we actually have K in units of MeV and Δm_0^2 in units of eV^2. If we wish to convert them to MKS units (that is, J^{-1}), we will have to multiply $\frac{K}{\Delta m_0^2}$ by a factor of $6.25x10^{24}$. Since $G_F = 4.5x10^{14} J^{-2}$ and $\frac{\int N_e(t)dt}{t}$ is in units of m^{-3}, the whole expression will be in units of $\left(\frac{s^2}{kgm^3}\right)^3$; so to make the expression dimensionless we need to multiply it by $(\hbar c)^3 = 3.16x10^{-77}\left(\frac{s^2}{kgm^3}\right)^{-3}$. Putting in all these conversion factors and integrating $N_e(t) = 10^{30}(10^6 t^3 - 4x10^4 t^2 + 100t + 4)$ from Fig. 4 and dividing it by t, we finally get:

$$2\theta_N(\mathrm{t}) = \arctan\left(\frac{1}{\cot(2\theta_0) - \frac{(1.26x10^{-7})K(2.5x10^5 t^3 - 1.3x10^4 t^2 + 50t + 4)}{\Delta m_0^2 \sin(2\theta_0)}}\right) \quad \{33\}$$

The transition probability given in {23} is $P_{trans} = \sin^2(2\theta_N(t))\sin^2(1.27\frac{\Delta m_N^2(t)}{K}L)$, where $\Delta m_N^2(t)$ is in eV^2, *K* in MeV and *L* in km. Using the relation *L*= *ct*/1000 and the relation between $\Delta m_N^2(t)$ and Δm_0^2 as given in {20}, we get:

$$P_{trans}(t) = \sin^2(2\theta_N(t))\sin^2\left(3.8x10^5 \frac{\Delta m_0^2}{K}\frac{\sin(2\theta_0)}{\sin(2\theta_N(t))}t\right) \quad \{34\}$$

where $2\theta_N(t)$ is given by {33}.

Fig. 9 gives a plot of the allowed values of Δm_0^2 and $\sin(2\theta_0)$. We shall take 4 results from the LMA (Large Mixing Angle) region together with several K values and plot $P_{trans}(t)$ in each of these cases. These plots can be found in Figs. 10-13.

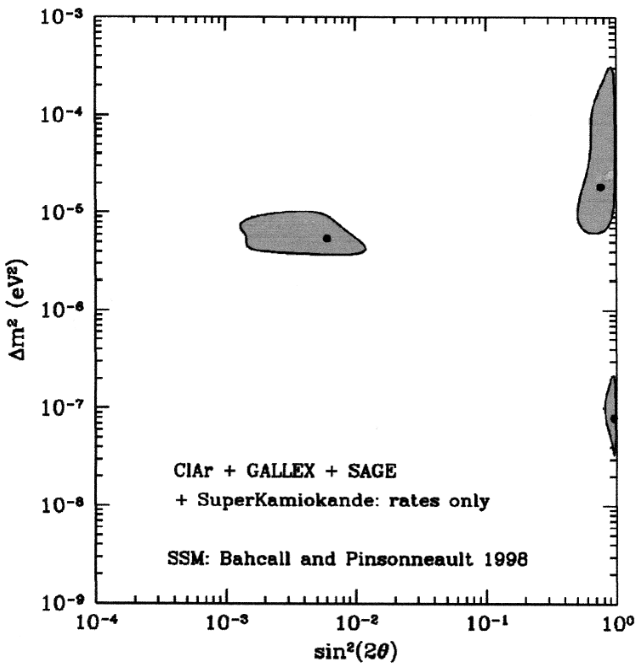

Figure 9. Plot of the allowed MSW solutions Δm_0^2 - $\sin(2\theta_0)$ parameter space as deduced from the results of the Homestake, Superkamiokande, Gallex and Sage experiments (taken from an article from Borexino's main website). The results we will be using will be taken from the Low Mixing Angle (LMA) region, *i.e.* the top left "block" on the plot.

Figure 10. Transition probabilities $P_{trans}(t)$ vs. time (s) at Δm_0^2 =1.8x10^(-5), $\sin(2\theta_0)$ =0.87 for neutrinos at 0.2 MeV, 0.5 MeV, and 0.8 MeV.

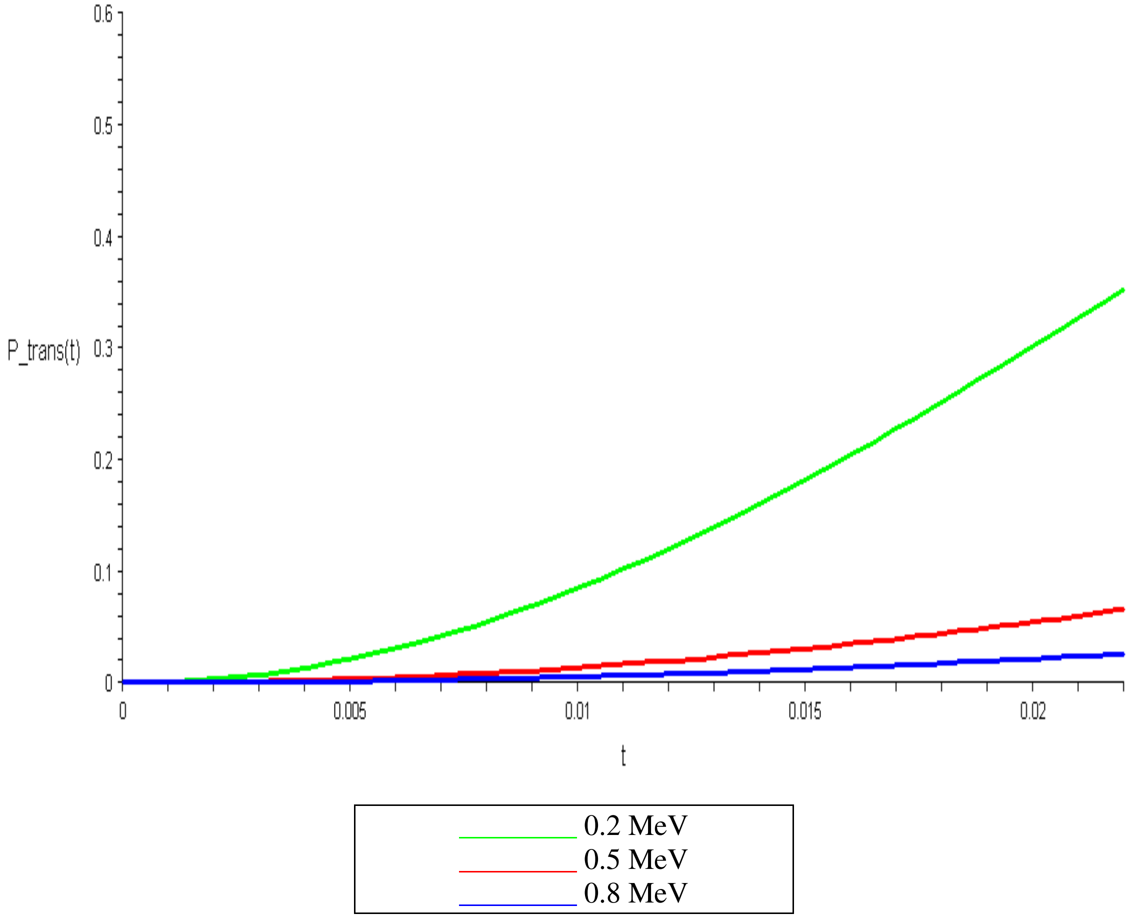

Figure 11. transition probabilities $P_{trans}(t)$ at Δm_0^2 =4x10^(-4), $\sin(2\theta_0)$ =0.95.

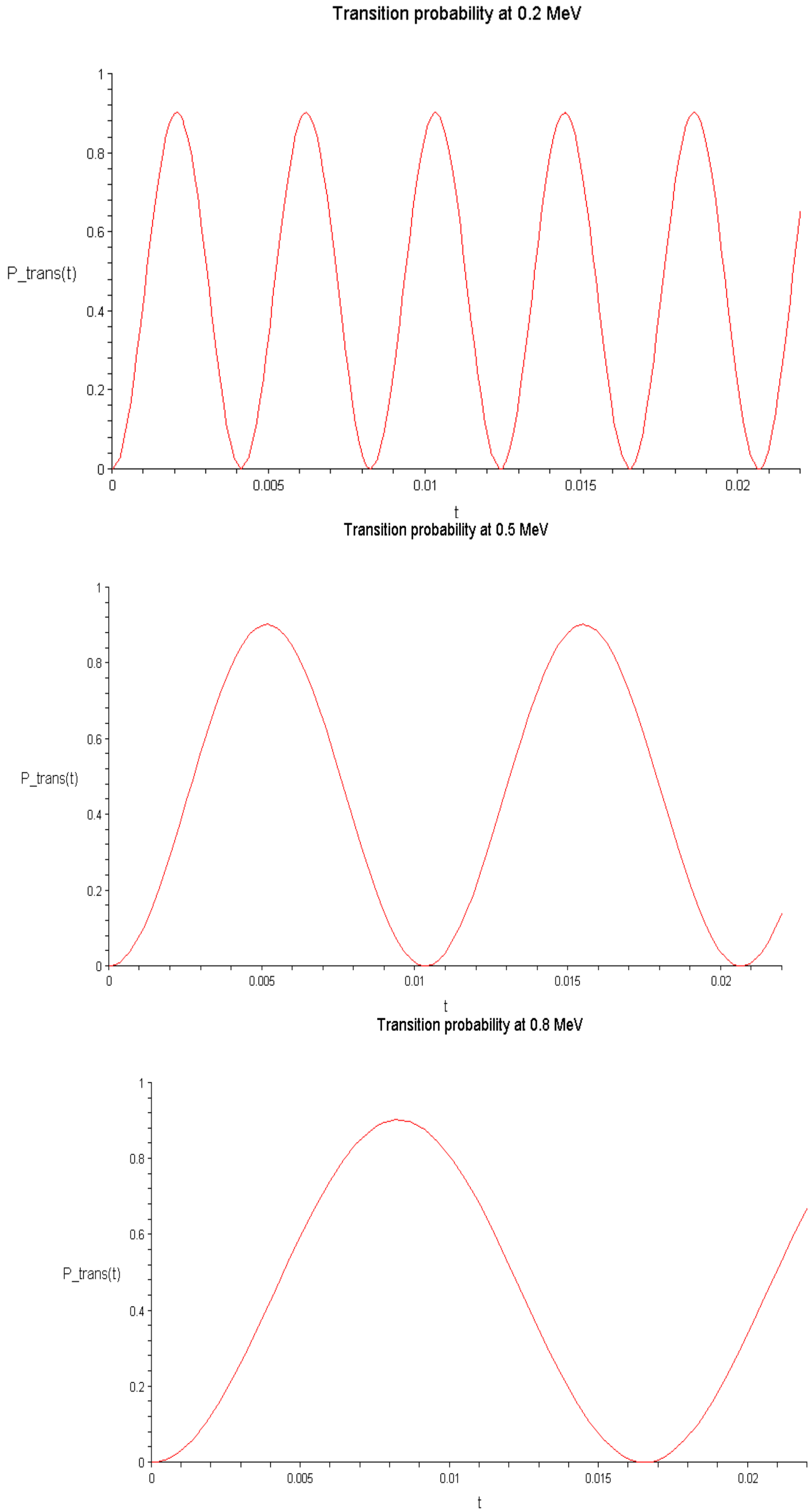

Figure 12. Transition probabilities $P_{trans}(t)$ at Δm_0^2=8x10^(-6), $\sin(2\theta_0)$=0.87 for neutrinos at 0.2 MeV, 0.5 MeV, and 0.8 MeV.

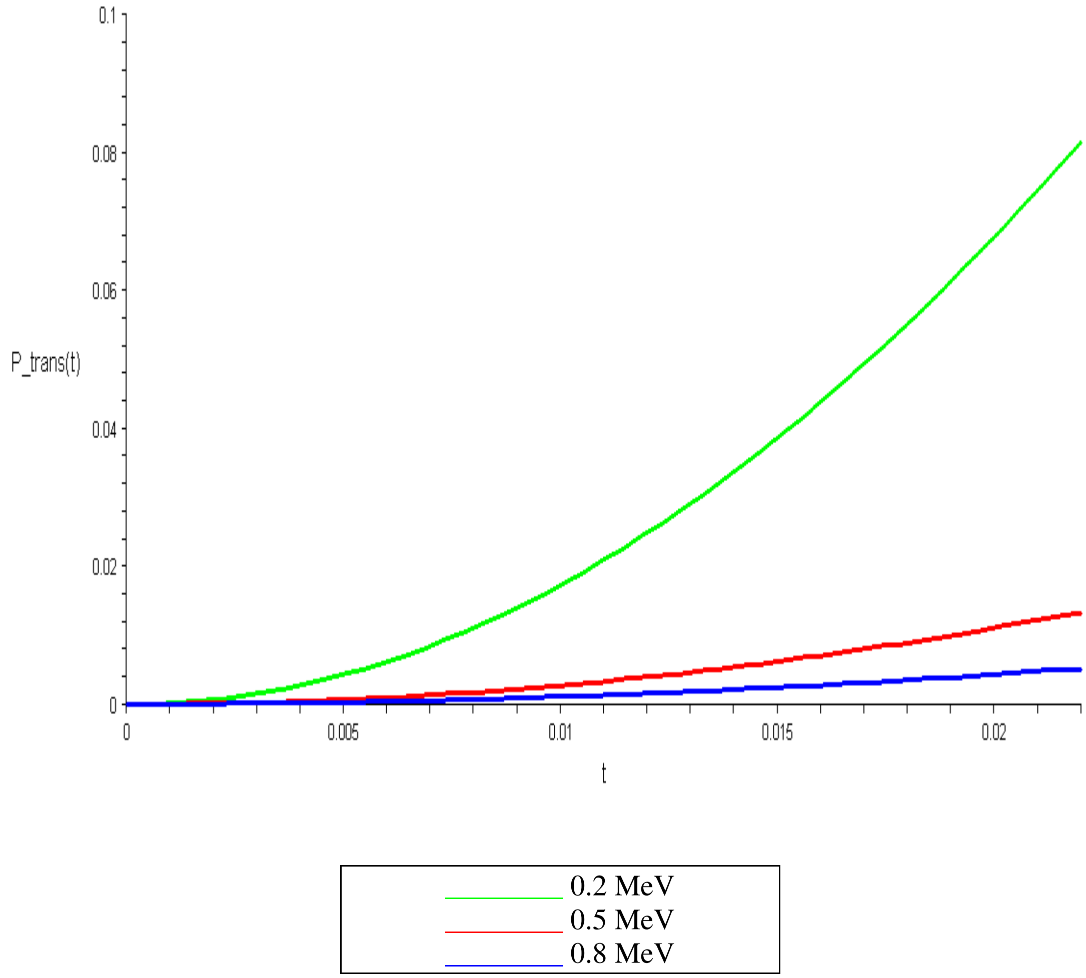

Figure 13. transition probabilities $P_{trans}(t)$ at Δm_0^2=10^(-4), $\sin(2\theta_0)$=0.86.

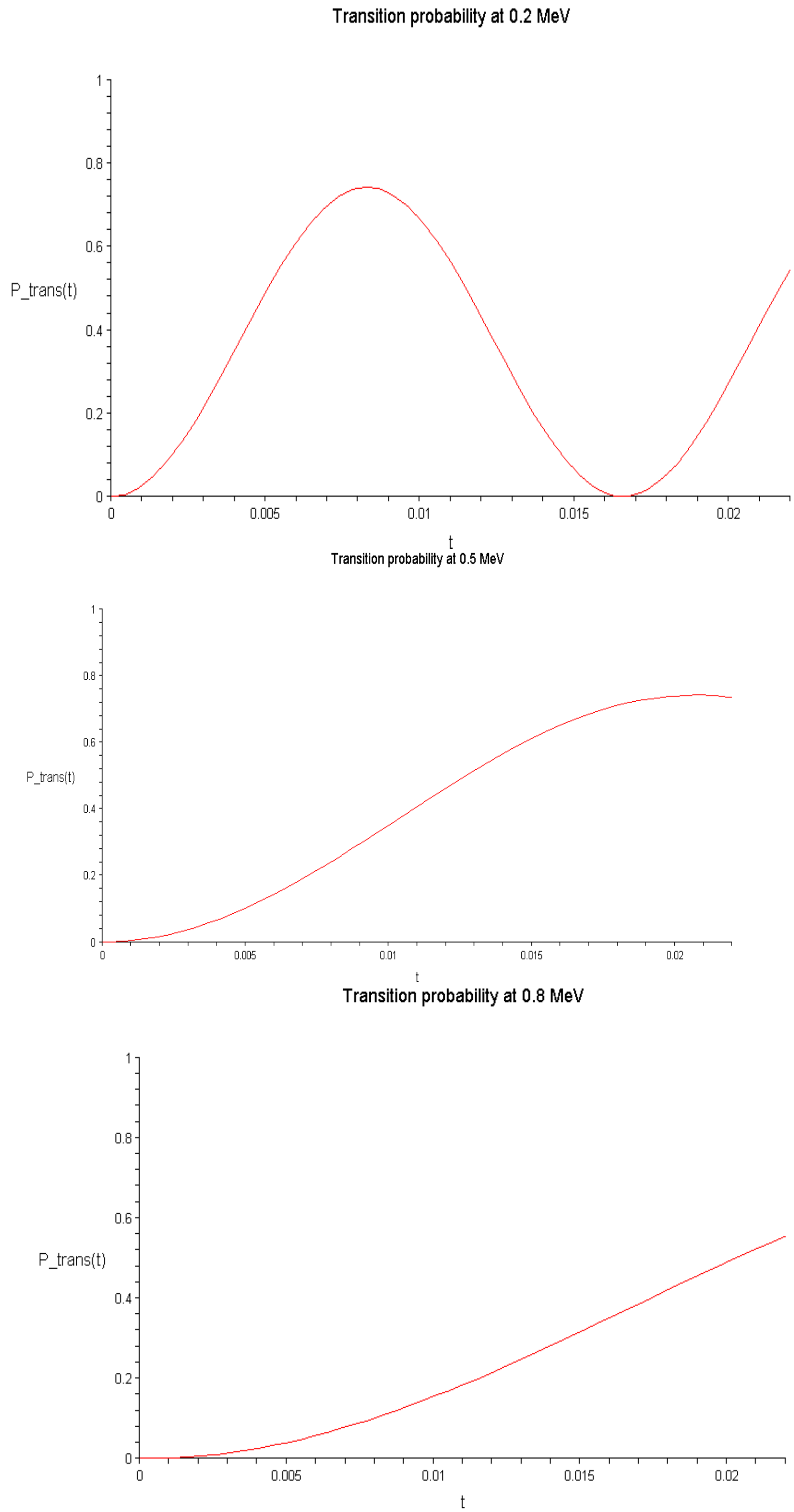

We can find the probability of ν_e produced in the core being detected as ν_μ by putting in $t = R_E / c$ into $P_{trans}(t)$. This probability varies with momentum (K) and Δm_0^2, as shown in Table 3 below, ranging from 0.0049 (for K, Δm_0^2 and θ_0 values of 0.8 MeV, $8x10^{-6} eV^2$ and 0.87, respectively) to 0.74 (for K, Δm_0^2 and θ_0 values of 0.5 MeV, $10^{-4} eV^2$ and 0.86, respectively).

Table 3. The various different transition probabilities for neutrinos with different values of momentum, Δm_0^2, and $\sin(2\theta)$

K(momentum)	(Δm_0^2, $\sin(2\theta)$)	Transition probability (P_{trans})	Figure reference (in Fig.16)
0.2 MeV	$(8\times10^{-6}, 0.87)$	0.0760	16.7
	$(4\times10^{-4}, 0.95)$	0.16	16.6
	$(1.8\times10^{-5}, 0.87)$	0.33	16.5
	$(10^{-4}, 0.86)$	0.45	16.4
0.5 MeV	$(8\times10^{-6}, 0.87)$	0.0125	16.11
	$(4\times10^{-4}, 0.95)$	0.0276	16.9
	$(1.8\times10^{-5}, 0.87)$	0.0600	16.8
	$(10^{-4}, 0.86)$	0.74	16.1
0.8 MeV	$(8\times10^{-6}, 0.87)$	0.0049	16.12
	$(4\times10^{-4}, 0.95)$	0.55	16.2
	$(1.8\times10^{-5}, 0.87)$	0.0247	16.10
	$(10^{-4}, 0.86)$	0.53	16.3

Finally, we are ready to plot the number of ν_μ detected by Borexino per year based on these probabilities. This time there is no background, though. These plots can be seen in Fig. 16 (Table 3 has listed the different probability values possible for neutrinos with different momentum and location in the LMA parameter space, with references to the figures in Fig. 16).

Figure 16: Figs. 16.1) through 16.l2) are plots of the number of ν_μ detected/year by Borexino for various transition probabilities, depending on the momentum and location in the LMA parameter space. Table 3 explained which figure refers to which data, and the note below further explains the pictures.

NOTE: The different colors in the figures refer to the various concentrations of K (some plots, especially of those neutrinos having low transition probabilities, do not have all colors pictured due to the very low number of neutrinos that can be detected at that concentration level):

7000 ppm

4000 ppm

2000 ppm

1000 ppm

500 ppm

Figure 16.1: Number of ν_μ detected/year for a transition probability of 0.74 (see table 3 above for the corresponding values of the parameters K, Δm_0^2 and $\sin(2\theta)$)

Number of ν_μ detected/year

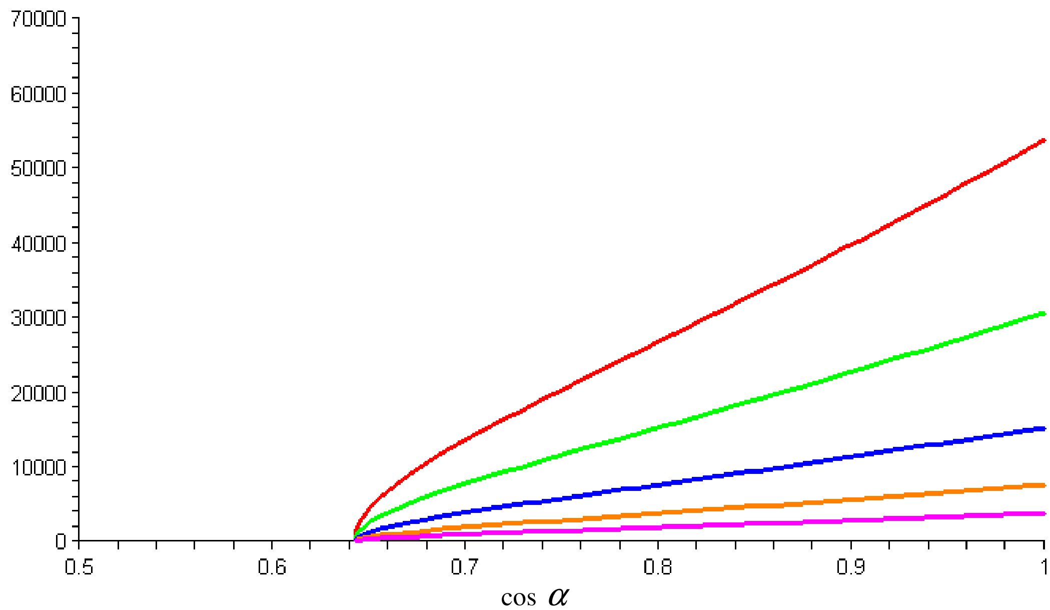

Figure 16.2: Number of ν_μ detected/year for a transition probability of 0.55 (see table 3 above for the corresponding values of the parameters K, Δm_0^2 and $\sin(2\theta)$)

Number of ν_μ detected/year

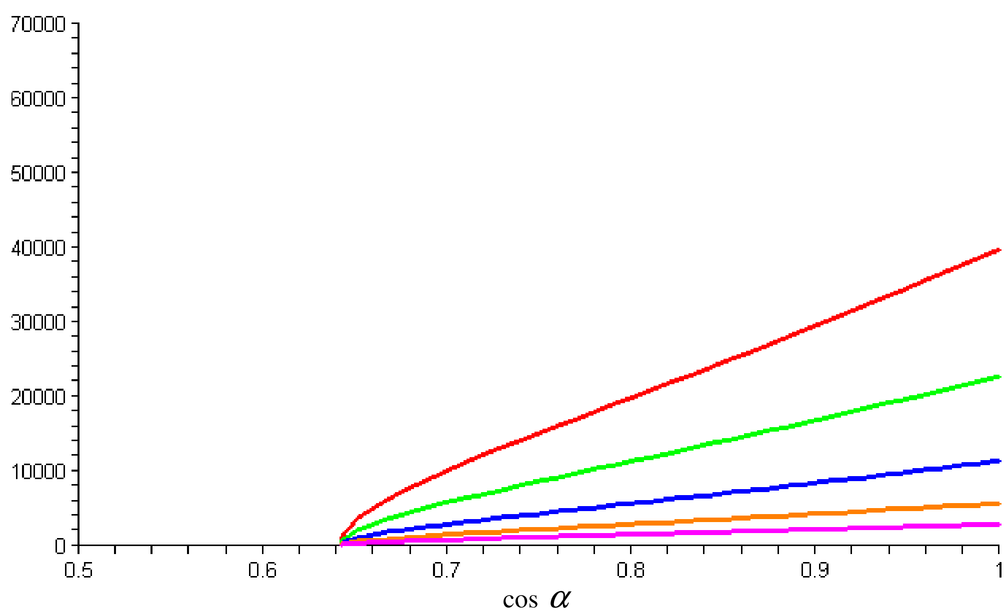

Figure 16.3: Number of ν_μ detected/year for a transition probability of 0.53 (see table 3 above for the corresponding values of the parameters K, Δm_0^2 and $\sin(2\theta)$)

Number of ν_μ detected/year

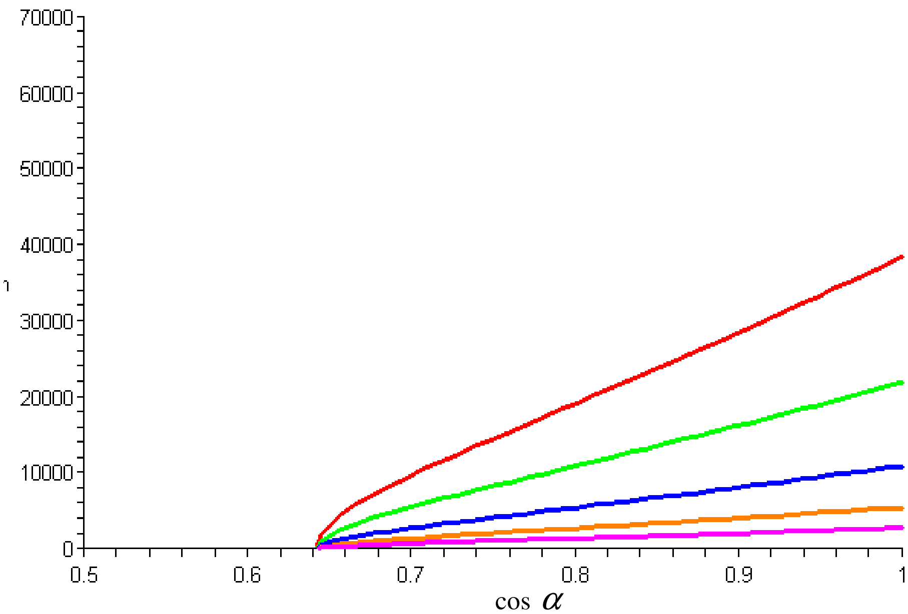

Figure 16.4: Number of ν_μ detected/year for a transition probability of 0.45 (see table 3 above for the corresponding values of the parameters K, Δm_0^2 and $\sin(2\theta)$)

Number of ν_μ detected/year

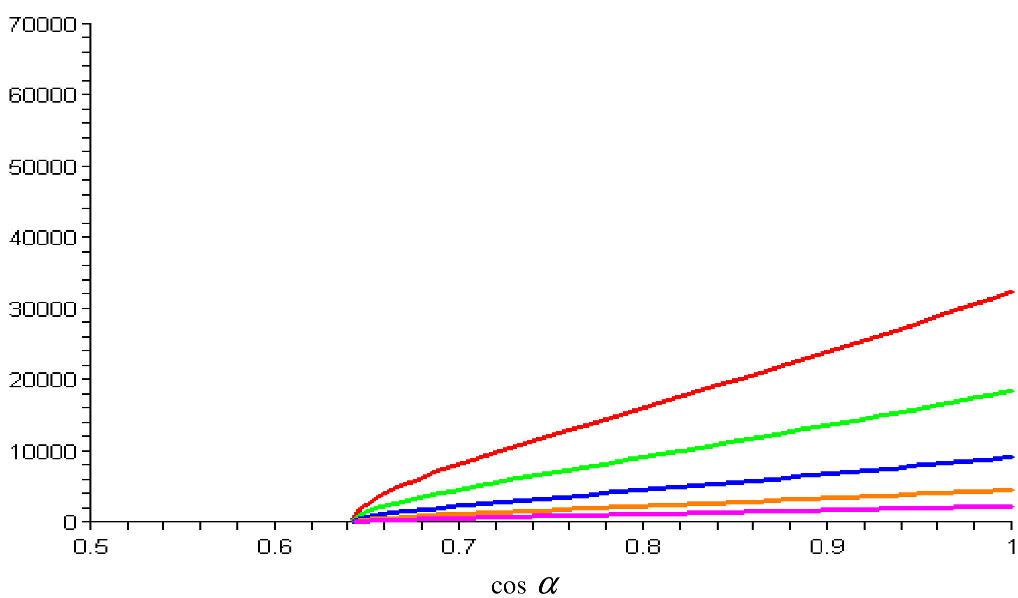

Figure 16.5: Number of ν_μ detected/year for a transition probability of 0.33 (see table 3 above for the corresponding values of the parameters K, Δm_0^2 and $\sin(2\theta)$)

Number of ν_μ detected/year

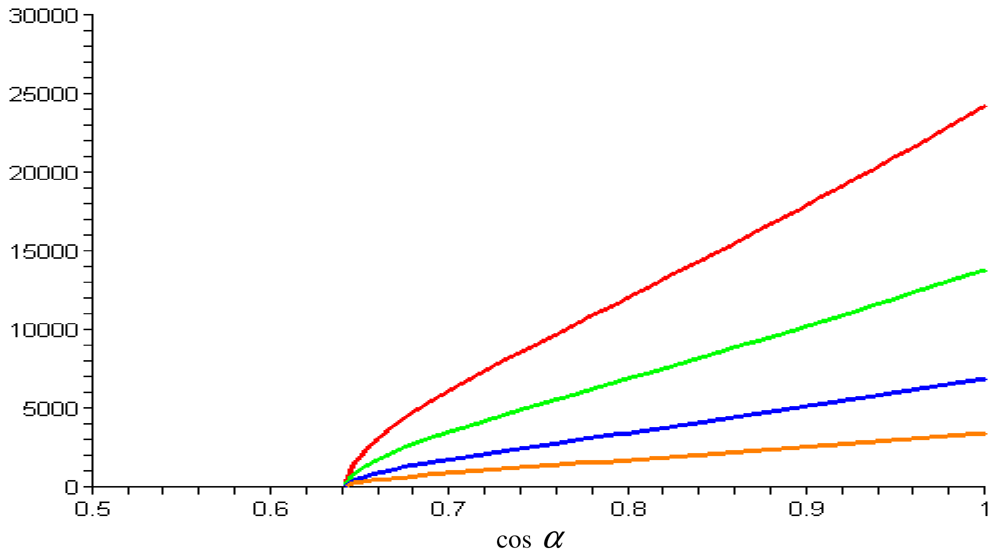

Figure 16.6: Number of ν_μ detected/year for a transition probability of 0.16 (see table 3 above for the corresponding values of the parameters K, Δm_0^2 and $\sin(2\theta)$)

Number of ν_μ detected/year

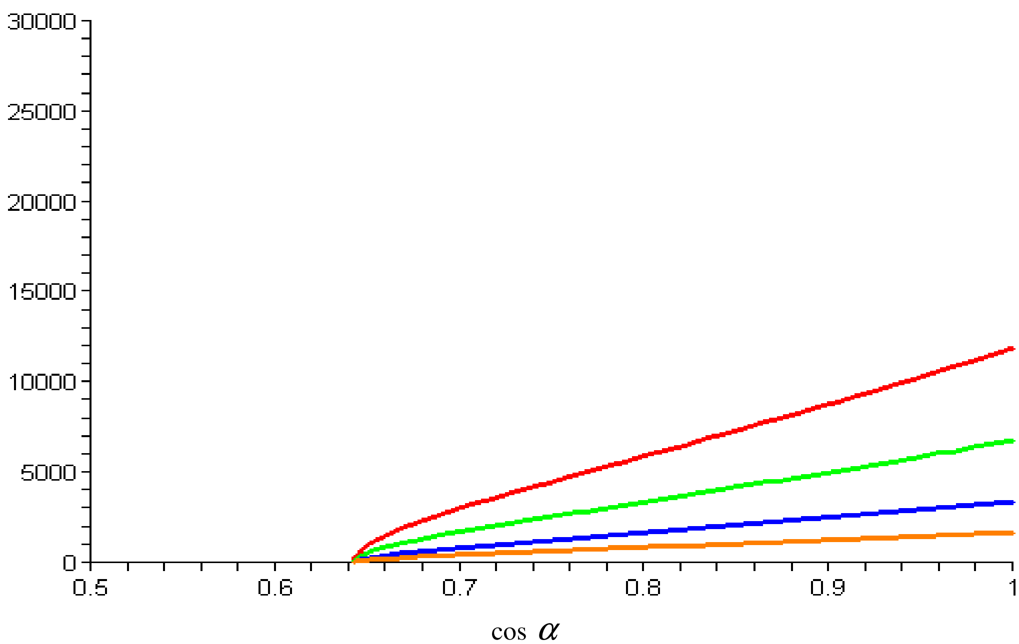

Figure 16.7: Number of ν_μ detected/year for a transition probability of 0.076 (see table 3 above for the corresponding values of the parameters K, Δm_0^2 and $\sin(2\theta)$)

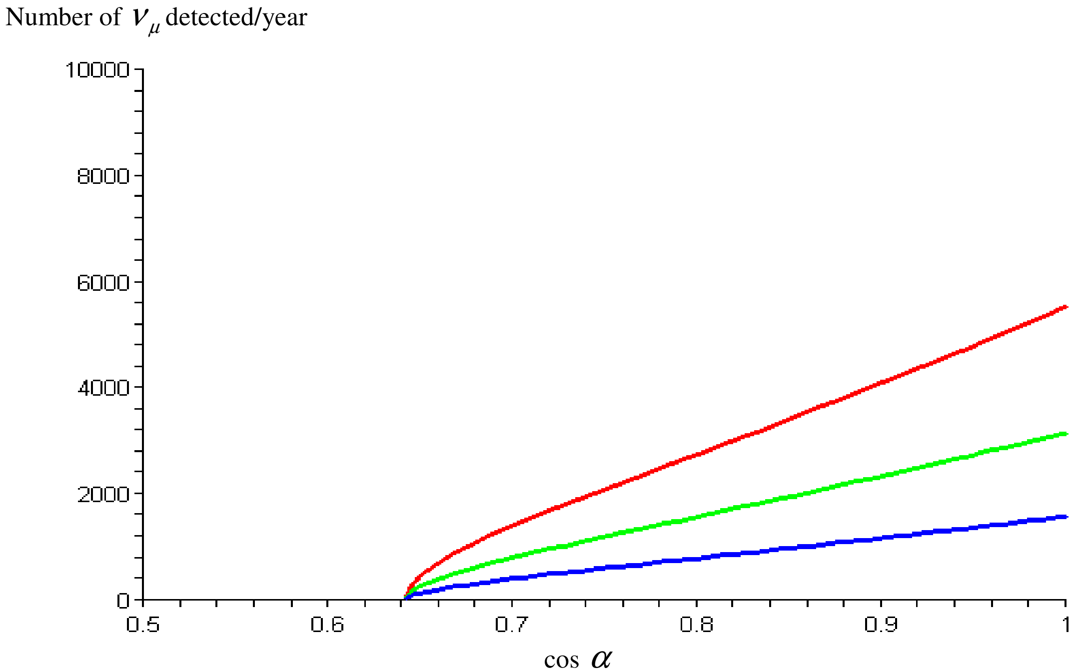

Figure 16.8: Number of ν_μ detected/year for a transition probability of 0.06 (see table 3 above for the corresponding values of the parameters K, Δm_0^2 and $\sin(2\theta)$)

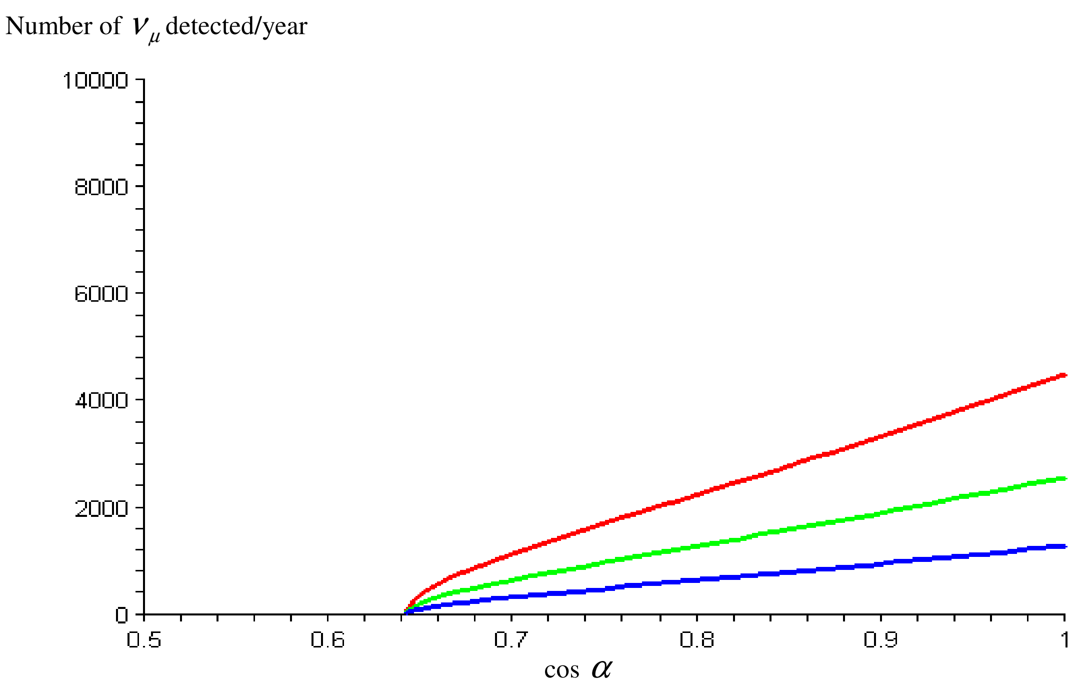

Figure 16.9: Number of ν_μ detected/year for a transition probability of 0.0276 (see table 3 above for the corresponding values of the parameters K, Δm_0^2 and $\sin(2\theta)$)

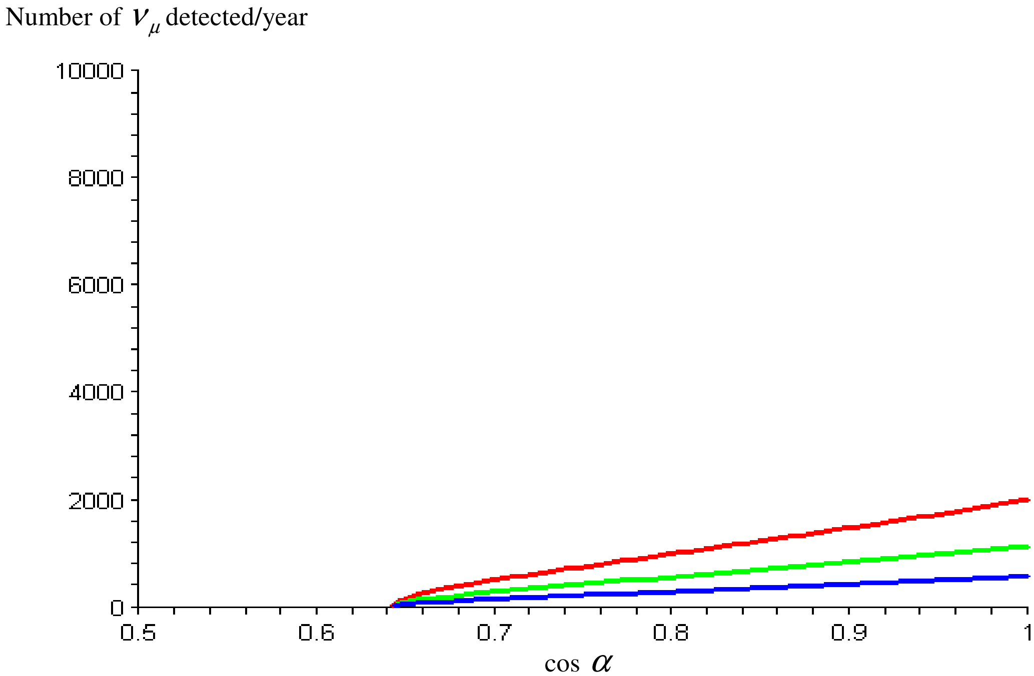

Figure 16.10: Number of ν_μ detected/year for a transition probability of 0.0247 (see table 3 above for the corresponding values of the parameters K, Δm_0^2 and $\sin(2\theta)$)

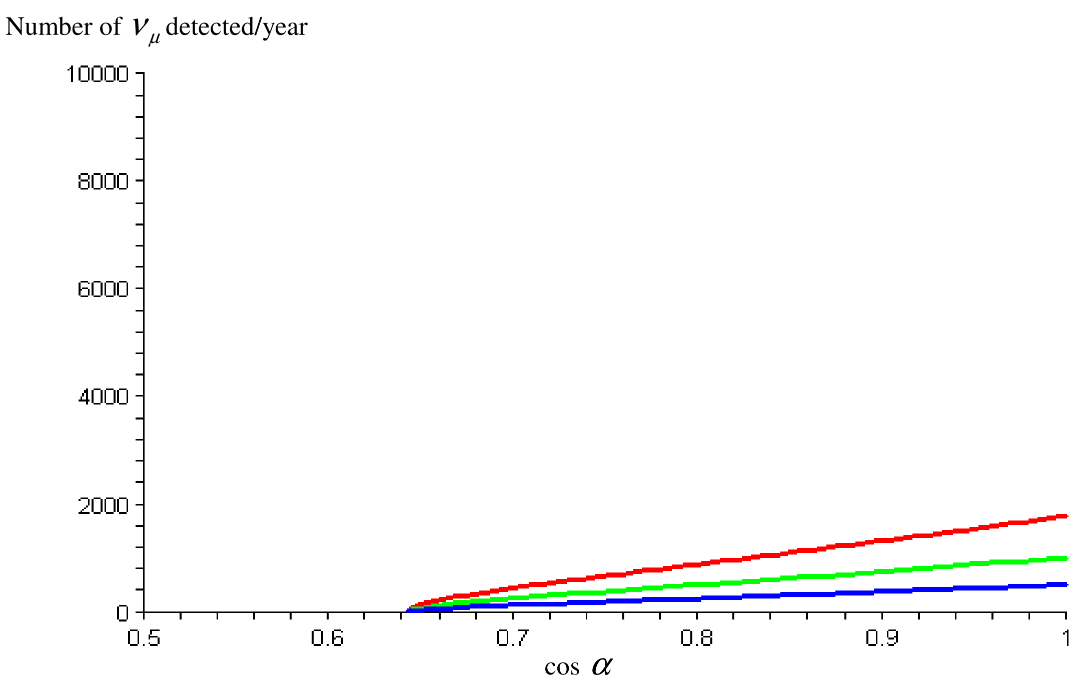

Figure 16.11: Number of ν_μ detected/year for a transition probability of 0.0125 (see table 3 above for the corresponding values of the parameters K, Δm_0^2 and $\sin(2\theta)$)

Number of ν_μ detected/year

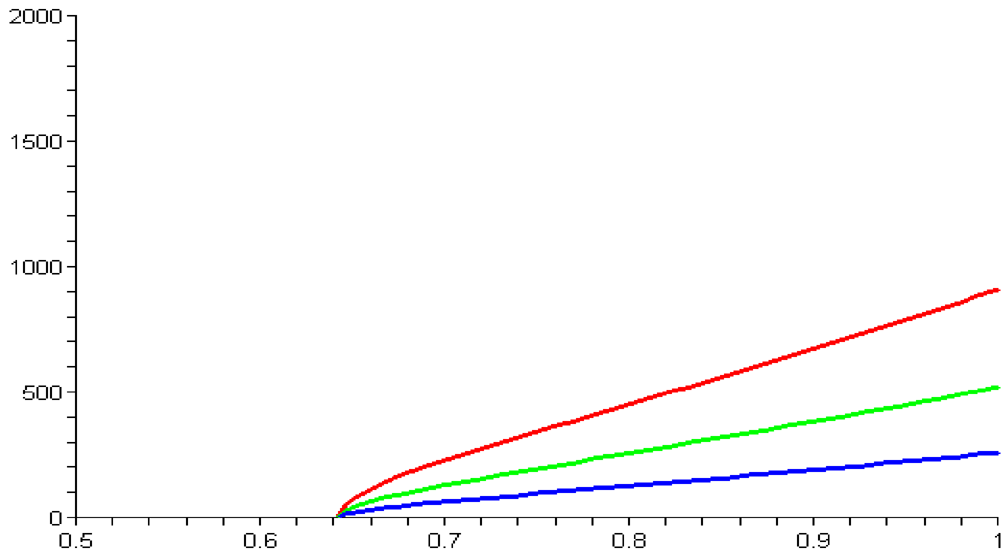

cos α

Figure 16.12: Number of ν_μ detected/year for a transition probability of 0.0049 (see table 3 above for the corresponding values of the parameters K, Δm_0^2 and $\sin(2\theta)$)

Number of ν_μ detected/year

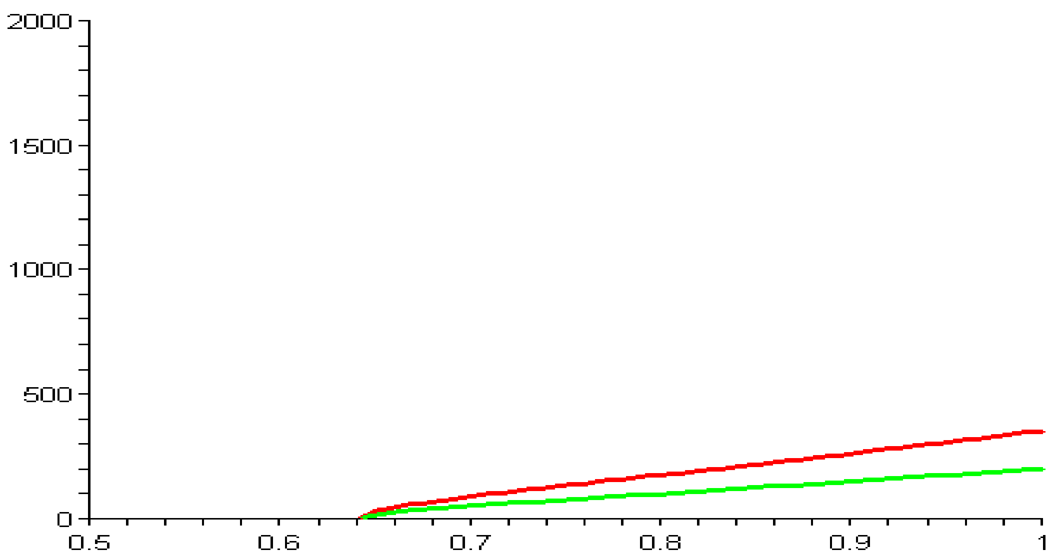

cos α

4) Conclusion

The behavior of neutrinos produced by $^{40}_{19}K$ in the earth's core has been analyzed, both in the oscillating and non-oscillating cases. The concentration of $^{40}_{19}K$ in the core is not yet known, so the analyses above have always focused on answering the question, "Approximately, what is the concentration at which there will be so few neutrinos produced that they are practically unobservable?"

If we ignore oscillations, Borexino will also produce (electron) neutrinos (called background) due to its impurities. Thus small concentrations of $^{40}_{19}K$ will produce so few neutrinos that they are indistinguishable from the background and are therefore unobservable; in the best case, a concentration of 800-900 ppm is necessary. In fact, a much higher concentration might be needed: in reality, neutrino and electron produced by a radioactive element will have various scattering angles, thus causing an uncertainty in the variable $\cos\alpha$ (see Fig. 3 for an illustration of the scattering angle α). This uncertainty will make neutrino detection more difficult (hence the possible requirement that $^{40}_{19}K$ concentration be higher than 800-900 ppm).

If we take neutrino oscillation (ν_e ->ν_μ) into account, there obviously will be no background. The probability that ν_e will be detected as ν_μ vary considerably depending on the values of ($\Delta m_0^2, \sin(2\theta_0)$) in the Low Mixing Angle (LMA) parameter space (see Fig. 9); it ranges from 0.0049 to 0.76 (see Table 3). Accordingly, the number of ν_μ detected/year also varies considerably; and thus the minimum required concentration of $^{40}_{19}K$ for ν_μ detection also varies considerably, depending on the values of

Δm_0^2 and $\sin(2\theta_0)$, see Fig. 16. For a transition probability value of 0.76 (Fig. 16.1), for example, a concentration of 500 ppm might still be acceptable; but for a probability value of 0.0049 (Fig. 16.12), it is very clear that a minimum concentration of 4000 ppm is required for neutrino detection. If we can narrow the allowed LMA parameter space (see Fig. 9) in the future, the resulting variation in transition probability might not be so enormous.

References

[1] Griffiths, David. "Introduction to elementary particles". Cornell University Press (1987).

[2] Mason, Brian. "Solar Neutrino Flavour Oscillations in the Moon". Senior Thesis. College of William and Mary, Spring 1994.

[3] Bernstein & Parke "Terrestrial long baseline neutrino oscillation experiments" Phys. Rev. D **44**, 7 pp.2069-2077 (1991).

[4] Firestone, R. "Table of Isotopes", Vol.1, 8th ed. Ed. V. Shirley. New York: John Wiley & Sons, Inc. (1996).

[5] Mantovani et al. "Antineutrinos from Earth: A reference model and its uncertainties". Phys. Rev. D **69**, 13001 (2004).

[6] Herndon, M. "Substructure of the inner core of the Earth". Proc. Natl. Acad. Sci. **93**, pp.646-648 (1996).

[7] Fields, B. and Hochmuth, K. "Imaging the earth's interior: the Angular Distribution of Terrestrial Neutrinos" [arXiv: hep-ph/0406001]

[8] Gessmann, C. and Wood, B. "Potassium in the Earth's core?" Earth Planet. Sci. Lett. **200**, pp.63-78 (2002).

[9] Lee, K and Jeanloz, R. "High-pressure alloying of potassium and iron: Radioactivity in the Earth's core?" Geophys. Res. Letters **30**, 23 (2003)

[10] Murthy, Westrenen, and Fei. "Experimental evidence that potassium is a substantial radioactive heat source in planetary cores". Nature **423**, pp. 163-165 (2003).

[11] Li J and Fei Y (2003). Experimental constraints on core composition, pp.521-546 in *The Mantle and Core* (ed. RW Carlson) Vol. 2 *Treatise on Geochemistry* (eds. H.D. Holland and K.K. Turekian), Elsevier-Pergamon, Oxford.

[12] http://borex.lngs.infn.it/about/borexinod.html
["The Borexino Detector"]

[13] Alimonti *et al*. "Borexino: A Large Scale Low Background Liquid Scintillation Detector: The Counting Test Facility at Gran Sasso."
http://www.lngs.infn.it/lngs_infn/index.htm?mainRecord=http://www.lngs.infn.it/lngs_infn/contents/lngs_en/research/experiments_scientific_info/experiments/current/borexino/CTF_EQP.htm

[14] http://cupp.oulu.fi/neutrino/nd-cross.html

[“The Ultimate Neutrino Page: Cross sections”]

[15] Alimonti *et al*., “Science and Technology of Borexino: A real time detector for low energy solar neutrinos”. Astropart. Phys. **16**, pp.205-234 (2002).

[16] DeBenedetti, Sergio. “Nuclear Interactions”. New York: John Wiley & Sons Inc., 1964.

[17] Bullen, K.E. “The Earth’s Density”. London: Chapman & Hall, 1975.

[18] Palme H. and O Neill H. (2003) Cosmochemical estimates on Mantle Composition , pp. 1-38 in *The Mantle and Core* (ed. RW Carlson) Vol 2 *Treatise on Geochemistry* (eds. H.D. Holland and K.K. Turekian), Elsevier-Pergamon, Oxford.